Microchimica Acta (2022) 189: 305
https://doi.org/10.1007/s00604-022-05404-4

ORIGINAL PAPER

On-bead DNA synthesis triggered by allosteric probe for detection of carcinoembryonic antigen

Min Ling[1] · Na Luo[1] · Lanyu Cui[1] · Yongqiang Cao[1] · Xueping Ning[1] · Jian Sun[1] · Xiaoping Xu[2] · Shengbin He[1]

Received: 21 April 2022 / Accepted: 3 July 2022 / Published online: 1 August 2022

Abstract

Sensitive quantification of protein biomarkers is highly desired for clinical diagnosis and treatment. Yet, unlike DNA/RNA which can be greatly amplified by PCR/RT-PCR, the amplification and detection of trace amount of proteins remain a great challenge. Here, we combined allosteric probe (AP) with magnetic bead (MB) for assembling an on-bead DNA synthesis system (named as APMB) to amplify protein signals. The AP is designed and conjugated onto the MB, enabling the protein biomarker to be separated and enriched. Once recognizing the biomarker, the AP alters its conformation to initiate DNA synthesis on beads for primary signal amplification. During the DNA synthesis, biotin-dATPs are incorporated into the newly synthesized DNA strands. Then, the biotin-labeled DNA specifically captures streptavidin (STR)–conjugated horseradish peroxidase (HRP), which is used to catalyze a colorimetric reaction for secondary signal amplification. By using carcinoembryonic antigen (CEA) as a protein model, the APMB can quantify protein biomarkers of as low as 0.01 ng/mL. The response values measured by APMB are linearly related to the protein concentrations in the range 0.05 to 20 ng/mL. Clinical examination demonstrated good practicability of the APMB in quantifying serum protein biomarker. The on-bead DNA synthesis could be exploited to improve protein signal amplification, thus facilitating protein biomarker detection of low abundance for early diagnosis.

Keywords Allosteric probe · Protein biomarker detection · Colorimetry · DNA synthesis · Magnetic separation · Carcinoembryonic antigen

Introduction

The development of proteome research has opened a new methodological era for diagnosis and therapy. Various proteins and their changes in expression levels are identified to serve as biomarkers for the occurrence and progressing of diseases [1–3]. Specially, the detection and quantification of a target protein at the level below 1 ng/mL is of great importance for the early disease screening, noninvasive diagnostic and bioscience research. For instance, clinical experiments demonstrated that carcinoembryonic antigen (CEA, a biomarker for a wide variety of tumors) concentration in serum was lower than 5 ng/mL in specimens obtained from healthy individuals [4]. The concentrations of β-amyloid (a biomarker for Alzheimer's disease) in tear and blood samples range from 1 to 10 pg/mL [5]. Cytokeratin 19 fragment (a biomarker for non-small cell lung cancer) presents in serum at the level of fg/mL [6]. Hence, trace protein analysis has become one of the research focuses currently.

Polymerase Chain Reaction (PCR) is an in vitro DNA synthesis technique for the amplification of a targeted DNA sequence based upon primer-directed polyreaction by a DNA polymerase. The PCR/RT-PCR and their derived methods are now widely used to detect DNA/RNA from various organisms, including viruses that cause Corona Virus Disease 2019 [7–11]. However, unlike DNA/RNA which can be greatly amplified by PCR/RT-PCR, the amplification and detection of trace amount of proteins remain a great

Min Ling, Na Luo, and Lanyu Cui contributed equally to this work.

✉ Shengbin He
comhsb@163.com

[1] Key Laboratory of Longevity and Aging-Related Diseases of Chinese Ministry of Education, Guangxi Colleges and Universities Key Laboratory of Biological Molecular Medicine Research, School of Basic Medical Sciences, Guangxi Medical University, Nanning, Guangxi 530021, People's Republic of China

[2] College of Chemistry, Fuzhou University, Fuzhou, Fujian 350108, People's Republic of China

challenge. For instance, enzyme-linked immunosorbent assay (ELISA), as a gold standard method for protein quantification, can hardly detect proteins of lower than 1 ng/mL [12]. Recently developed techniques, such as electrochemical assays [13, 14] and Surface-enhanced Raman scattering [15], can lower the detection limit to 0.01–0.1 ng/mL. Yet, the poor repeatability and quantifiability of the methods have confined themselves to the laboratory. Therefore, it is urgently needed to explore new techniques that can detect protein biomarkers of less than 1 ng/mL, with specificity, repeatability and quantifiability comparable to ELISA.

Here, we utilize an allosteric probe (AP) conjugated on nano-magnetic beads (MBs) for the identification and signal amplification of protein biomarkers, which is named as APMB system. The AP is a single-stranded 49-nt DNA, with three sequences to form a hairpin structure through partially base pairing. The hairpin structure transforms to a linear structure as a response to target proteins, thus exposing primer binding sites for DNA synthesis. During the DNA synthesis on the magnetic beads, biotinylated deoxyribonucleoside triphosphoric acid (biotin-dATPs) are incorporated into the newly synthesized DNA strands, generating numerous biotin-labeled double-stranded DNAs (dsDNAs) for primary signal amplification. The biotin-labeled dsDNAs on the magnetic beads specifically bind to the horseradish peroxidase conjugated streptavidin (HRP-STR), which is used to catalyze the colorimetric reaction of tetramethylbenzidine (TMB) for secondary signal amplification. By using CEA as a model protein, the advantages of the APMB system against traditional ELISA with respect to sensitivity, repeatability and quantifiability were demonstrated.

Experimental section

Reagents and chemicals

Bsm DNA Polymerase (large fragment), carboxyl magnetic beads (300 nm), HRP-STR, FITC-conjugated Streptavidin (FITC-STR), digoxin, digoxin monoclonal antibody (MID0302), and biotin-dATP, SYBR Green, streptavidin conjugated PE-Alexa Fluor™ 647 (PE-AF647-STR) were purchased from Thermofisher (Massachusetts, USA). Carcinoembryonic antigen (CEA), glucose, urea and bovine were purchased from Solarbio Life Sciences (Beijing, China). All allosteric probes (custom-designed), primers (custom-designed), and other chemical reagents for DNA synthesis were purchased from Sangon Biotechnology Co. Ltd (Shanghai, China). The antibodies and chemical reagents for ELISA were purchased from Sino Biological (Beijing, China). All the chemicals and biological materials were of analytical grade.

Design of allosteric probes with different complementary length

Fluorescent-labeled allosteric probes (Supplementary Table S1) were dissolved in 2 × TAE buffer (containing 80 mM Tris, 40 mM acetic acid, and 4 mM EDTA), and diluted to 10 μM. Before being used, allosteric probe solutions were incubated at 60 °C for 3 min and cooled to room temperature to ensure that the APs were correctly folded into a hairpin structure. Mix 20 μL allosteric probe solution with 20 μL CEA solution (80 ng/mL). The mixture was subjected to dissociation curve analysis by StepOnePlus Rea-Time PCR System with temperature ranging from 15 to 85℃ and a gradient of 1℃.

Design of primers with different complementary length

Prepare a 25 μL DNA synthesis mixture, with 1U DNA Ploymerase (large fragment), 2 μM allosteric probe, 2 mM primers of different complementary length (as shown in Supplementary Table S2), 1.4 mM dNTP mix, 6 mM $MgCl_2$, and CEA (80 ng/mL). The mixture was incubated at 37 °C for 60 min. The synthesized double-stranded DNA was detected by electrophoresis with 4.5% agarose gel.

To investigate the effect of CEA on the initiation of DNA synthesis, the CEA (dissolved in pure water) concentrations were controlled to range from 0 to 160 ng/mL. For biotin labeling, biotin-dATP with final concentration ranging from 0 to 1.4 mM was added to the synthesis mixture. The insertion of biotin-dATP into dsDNA was certificated by adding 20 μL streptavidin solution (0.5 mg/mL) to the synthesis mixture before electrophoresis analysis.

Preparation of AP conjugated magnetic beads

Details for preparation of anti-digoxin antibody–conjugated magnetic beads are provided in Supplementary protocol 1. Pipe 50 μL of anti-digoxin antibody conjugated magnetic beads solution (10 mg/mL) into a microcentrifuge tube. Place the tube into a magnetic stand, followed by collecting the beads and discarding the supernatant. Re-suspend the beads in 100 μL of TAE buffer, and add 100 μL of digoxin-labeled AP solution (10 mM, dissolved in pure water). The solution was incubated at room temperature on a rotator for 60 min. Wash the beads twice with TAE buffer (1 mL each time) by magnetic separation, and then re-suspend the beads in 500 μL of TAE buffer. Place the AP-conjugated magnetic beads at 4 °C for later use. The coupling efficiency of the AP on the magnetic bead was calculated to be 73.1% according

to the ultraviolet spectrophotometer analysis of AP solutions after magnetic bead separation.

Characterization of the AP conjugated magnetic beads

The formation of the antibody conjugated magnetic beads and the combination of the APs onto the beads were verified by dynamic light scattering (DLS, Malvern, UK) through Zeta-potential analysis. The on-bead DNA synthesis was certificated by fluorescence staining of the magnetic beads with FITC conjugated streptavidin (FITC-STR) targeted to the biotinylated DNA. Specifically, 20 µL FITC-STR solution (0.5 mg/mL) was added to 100 µL magnetic beads (0.25 mg/mL) in the tube. The suspension was incubated for 20 min at room temperature. After magnetic separation, the magnetic beads were resuspended with 500 µL TAE buffer and subjected to flow cytometry analysis as described by Sun et al. [16]. The magnetic beads with DNA on its surface were further verified via laser-scanning confocal microscopy and transmission electron microscopy (FEI Tecnai G2 F30).

Detection of CEA by APMB system

Pipe 25 µL AP-conjugated magnetic beads solution (1 mg/mL) into a microcentrifuge tube. Then, 25 µL 4 × binding buffer (TAE buffer) and 50 µL serum sample were added to the tube. Mix the solution in the tube thoroughly, and incubate it for 10 min. Magnetic separation was carried out to discard the supernatant. Next, the on-bead DNA synthesis reaction was performed with Bsm DNA Ploymerase (large fragment, 4U), primer (2 µM), dNTP mix (1.4 mM each), biotin-dATP (0.28 mM), and $MgCl_2$ (6 mM) at 33 °C for 30 min in a 100 µL reaction system. For specificity tests, fixed amount of serum-derived interferents (BSA, skim milk, KCl $NaHCO_3$, glucose, and $MgSO_4$) were spiked into 100 mL pure water, respectively, to prepare interferents. After the DNA synthesis, magnetic separation was carried out to discard the supernatant. Wash the beads twice with TAE buffer, followed by adding 100 µL TMB substrate. After chromogenic reaction for 5 min, the mixtures were detected by a microplate reader for recording absorbance at 450 nm (OD_{450}). The response values of colorimetric reaction directly reflected the original concentration of the target analyte for CEA values in the range of 0.01–20 ng/mL. For CEA values above 20 ng/mL, the serum was diluted into pure water, and recoveries were calculated by multiplying the dilution ratio.

For validation test, clinical samples of unknown amount of CEA from healthy donors were detected by traditional ELISA and APMB system, respectively. Informed written consents were obtained from the donors and the collection of blood samples was approved by the Ethics Committee of the First Affiliated Hospital of Guangxi Medical University.

Detection of CEA by ELISA assay

The ELISA assays were carried out according to the typical sandwich ELISA method as described by Sun et al. [4]. More detailed protocol is provided in Supplementary protocol 2.

Results and discussion

Work principle of the APMB system

Figure 1 shows the assembling of APMB and how it works. A specific allosteric probe (AP) was conjugated to the magnetic bead through digoxin/antidigoxin antibody interaction. There are three sequences in the AP to form a hairpin structure: a recognition sequence (green) to identify target protein, a complementary sequence (red) to provide a concealed primer binding site, and a linking sequence (blue). The 3′ end of the AP was labeled with digoxin so that it could be conjugated to the anti-digoxin antibody modified magnetic bead [17].

In step 1, the AP-conjugated magnetic beads identify target proteins from the serum sample and enrich them through magnetic separation. When there was no target protein, the primer binding site of the AP was concealed by its hairpin structure, and DNA synthesis was blocked. When target protein appeared, the recognition domain specifically bind with target protein, resulting in the switch of the AP from hairpin structure to active linear structure [18, 19]. Consequently, the primer binding site was available for the primer to initiate template-dependent primer extension reaction, as show in step 2. Due to the polymerase extension reaction, the binding ability between the two complementary sequences increased rapidly, to a point where it exceeded the binding ability between CEA and AP. As a result, the target protein was displaced by the new DNA strand and entered to the next cycle for primary signal amplification [18], as shown in step 3 to step 4. During the DNA synthesis, biotin-dATP is randomly incorporated into the dsDNA. Finally, in step 5, streptavidin-conjugated horseradish peroxidase (HRP-STR) is used to identify the biotinylated dsDNA on the beads and conduct enzymatic reaction, thereby generating colored products for secondary signal amplification.

Design of AP with specific response to target protein

We used carcinoembryonic antigen (CEA), a biomarker of multiple cancers [13, 20–22], as a protein model for testing. The DNA sequence of the recognition sequence (5′ATACCA

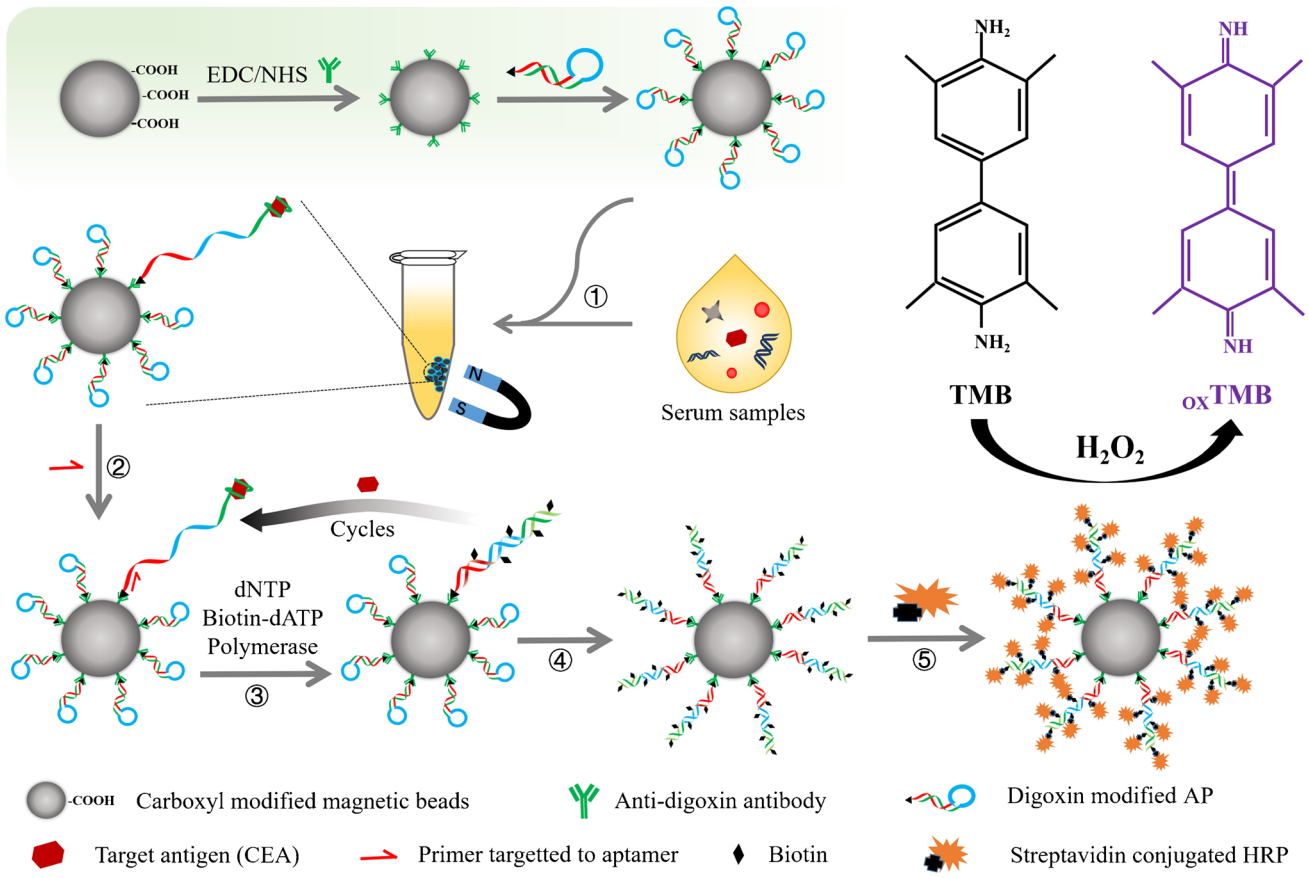

Fig. 1 Work principle of the APMB system for protein detection. Step 1 to 5 describes on-bead DNA synthesis triggered by allosteric probe (AP)

GCTTATTCAATT 3′) in AP was reported by Tabar, H. et al. [23]. We chose this sequence as recognition module based on its high affinity against CEA, with a dissociation constant of 0.69 nM. A good specificity of the sequence to CEA was demonstrated by several research groups [24–26].

To demonstrate the switch of the AP from hairpin structure to linear structure, the AP was labeled with a fluorochrome (FAM) at the complementary terminal and a quencher (BHQ1) at the recognition terminal, as depicted in Fig. 2a. Without CEA, the hairpin AP brought the FAM and BHQ1 close to each other by base pairing, resulting in quenched fluorescence. In the presence of CEA, the AP transformed to linear structure thus keeping the FAM far away from the BHQ1 and resulting in fluorescence recovery.

In the AP, the length of base pairing plays an important role in maintaining the stability of the hairpin structure. A desired hairpin AP should have enough stability to resist background interference while maintain responsiveness to the target protein. In order to acquire such an AP, six APs (AP5, AP9, AP11, AP13, AP15, and AP17) with various complementary length were designed (the sequences are listed in Supplementary Table S1). Figure 2b and Supplementary Fig. S1 show the fluorescence response of these APs with 80 ng/mL CEA under different temperatures. The fluorescence signal of APs increased after incubation with CEA. At low temperatures, the APs showed reduced fluorescence background (without CEA) with longer complementary sequence. When the complementary sequence shortened, the fluorescence signals of APs, as response to CEA, were enhanced. For all the APs, the response sensitivity weakened sharply when the temperature increased to the points where lots of the complementary sequences were melted. For melted APs, fluorescence signal decreased with the increase of temperature. Because high temperature would increase the vibrational relaxation and excited-state interactions of the fluorescent molecules, both of which would result in fluorescence quenching [27]. We defined the ratio of maximum fluorescence signal of CEA response curve to the fluorescence background at the same temperature point as signal-to-background ratio (S/N), as shown in Fig. 2b(II). The optimal AP with highest S/N was AP11, as shown in Fig. 2c. These results confirmed that the AP11 could successfully binds to CEA and switches to its active configuration, with an optimized temperature of 33℃. Laser

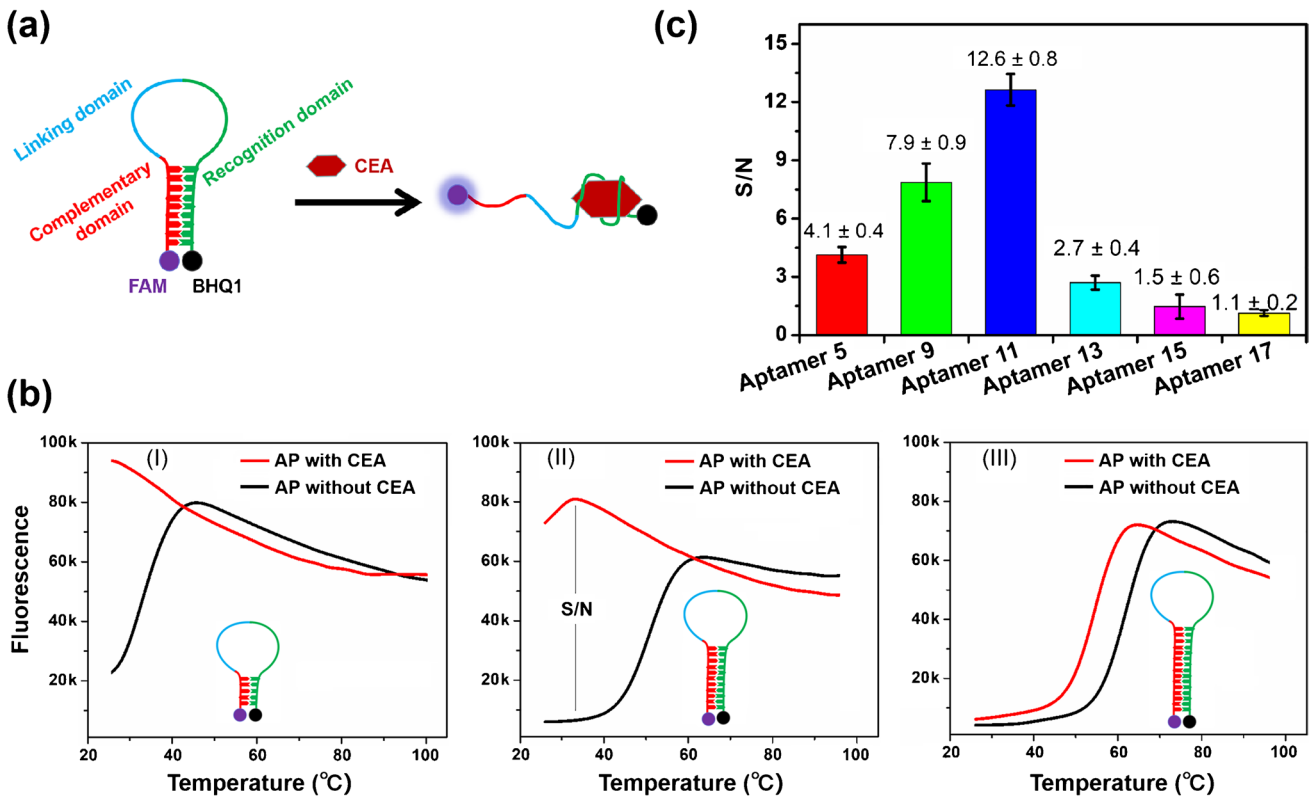

Fig. 2 Design of AP with response to target protein (CEA). (a) Two-dimensional structure of the AP and its transformation. (b) Fluorescence response of various APs in the presence of 80 ng/mL CEA under different temperatures. (I), (II), and (III) represent APs with complementary lengths of 5 bp, 11 bp, and 15 bp, respectively. (c) Signal-to-background ratio (S/N) of the APs in response to 80 ng/mL CEA

scanning confocal microscope analysis further demonstrated the switch of the AP 11 from hairpin structure to linear structure, as shown in Supplementary Fig. S2. Therefore, AP11 is selected for the subsequent experiments to establish the APMB system.

In vitro DNA synthesis triggered by AP as response to CEA

Agarose gel electrophoresis (AGE) analysis was performed to demonstrate the CEA-triggered DNA synthesis, and to verify the successful insertion of biotin into the synthesized dsDNA, as shown in Fig. 3a. Four primers named primer 6, primer 8, primer 10, and primer 12, with varied lengths (6, 8, 10, and 12 nt respectively) were designed and their specific sequences were shown in Supplementary Table S2. As shown in Fig. 3b, without target protein (CEA), the hairpin AP could not unfold even under the addition of primer 6 (lane *control 6*), primer 8 (lane *control 8*), or primer 10 (lane *control 10*); therefore, no dsDNAs were synthesized. However, when the primer length increased to 12nt, a fraction of the AP could be unfolded by the primer through strand displacement reaction, thus generating non-specific amplification (Fig. 3b lane *control 12*). When CEA (80 ng/mL) was introduced to the AP, primers with a length over 6nt bound to the unfolded AP and DNA synthesis was initiated by the polymerase to generate dsDNA with larger molecular weight (Fig. 3b Lanes *primer 8*, *primer 10*, and *primer 12*). Among the tested primers, primer 10 demonstrated both the best specificity and the highest amplification efficiency.

We further evaluated the quantifiability of AP-triggered DNA synthesis at CEA concentrations ranging from 0 to 160 ng/mL. The results in Fig. 3c demonstrated good performance of the optimized AP and primer for the linear amplification of CEA molecules, with a naked-eye detection limit of 5 ng/mL. Next, we labeled the newly synthesized DNA with biotin by using biotin-dATP as substrate for DNA synthesis. Figure 3d shown the amplification results in the presence of varied biotin-dATP contents. The resultant products were incubated with streptavidin (STR) before AGE analysis. In the absence of biotin-dATP, the synthesized dsDNA fragments showed small molecular weight (lane *0*); while in the presence of biotin-dATP, the dsDNA fragments showed larger molecular weight due to the binding of the biotin-dsDNA to streptavidin. As the biotin-dATP increased, more

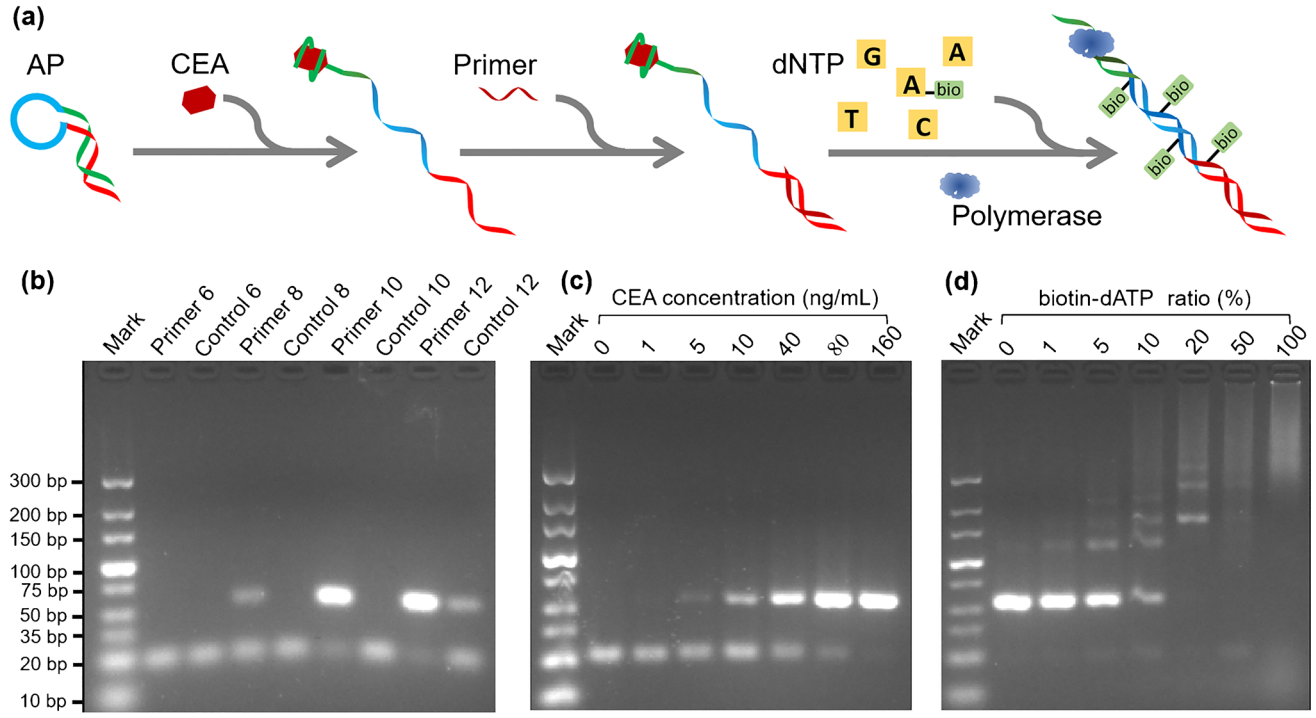

Fig. 3 Electrophoretic analysis of the feasibility of APMB for CEA detection. (a) Schematic diagram of in vitro DNA synthesis triggered by primer and CEA. (b) DNA synthesis with 80 ng/mL CEA for different primers. Primer 6, primer 8, primer 10, and primer 12 represent primers with lengths of 6nt, 8nt, 10nt, and 12nt, respectively. For controls, no CEA were present. (c) DNA synthesis with different CEA contents for primer 10. (d) DNA synthesis with different biotin-dATP contents and a CEA concentration of 80 ng/mL. The synthesized DNA was incubated with streptavidin before electrophoretic analysis

and more dsDNA fragments were trapped in the front of the agarose gel, indicating more and more biotin-dATPs were incorporated into the dsDNA. When the biotin-dATP ratio increased to 50%, the DNAs tended to aggregate. We chose 20% as the optimal biotin-dATP ratio, because at this point, all the dsDNA fragments were successfully labeled with biotin, and meanwhile the dsDNA fragments maintained as dispersive as possible. These results indicated that the biotin-labeled DNA can bind to HRP-STR in the downstream reaction for secondary signal amplification.

Characterization of on-bead DNA synthesis

It is worth mentioning that the complex components in biological samples may inhibit the enzymatic reactions, hindering both DNA synthesis and colorimetric reaction. The on-bead DNA synthesis was able to separate the target proteins from the samples, which also facilitated the purification of HRP-STR-biotin-dsDNA from the reaction matrix. Hence, we conjugated the AP to the magnetic bead (MB) through digoxin/antidigoxin antibody interaction. As shown in Fig. 4a, the zeta potential of MB decreased from − 30 to − 40 mV after conjugation with anti-digoxin antibody, and further dropped to − 55 mV after conjugation with the AP; because both the anti-digoxin antibody and oligonucleotide AP are negatively charged. The size distribution of MB remained unchanged (around 300 nm) after conjugation with either antibody or AP (Fig. 4a and b). However, after DNA synthesis and incubation with HRP-STR, the MBs tended to aggregate to form larger sizes, as shown in Fig. 4b. This aggregation can be ascribed to the binding of HRP-STR with biotin-dsDNAs at multiple sites on the beads, as one STR molecule can binds four biotin molecules [28]. Transmission electron microscopy further confirmed the aggregation of the beads after adding HRP-STR, as shown in Fig. 4c. Flow cytometry analysis with FITC-STR fluorescence staining was carried out to verify the successful DNA synthesis on the beads. As shown in Fig. 4d, the beads carrying biotin-dsDNAs showed heterogeneous fluorescence after incubation with FITC-STR, suggesting the successful on-beads DNA synthesis and the insertion of biotin molecules into the on-beads dsDNA.

Figure 5 shows confocal laser scanning microscope analysis of the beads. Either SYBR Green targeted to dsDNA or streptavidin conjugated PE-Alexa Fluor™ 647 (PE-AF 647-STR) targeted to biotin-labeled DNA was used for MB staining. The Anti.-MB (antibody conjugated MB) failed to initiate DNA synthesis due to the lack of AP modification, thus showing no fluorescence (Fig. 5 a1 and a2). Because the hairpin AP itself formed a complementary dsDNA of

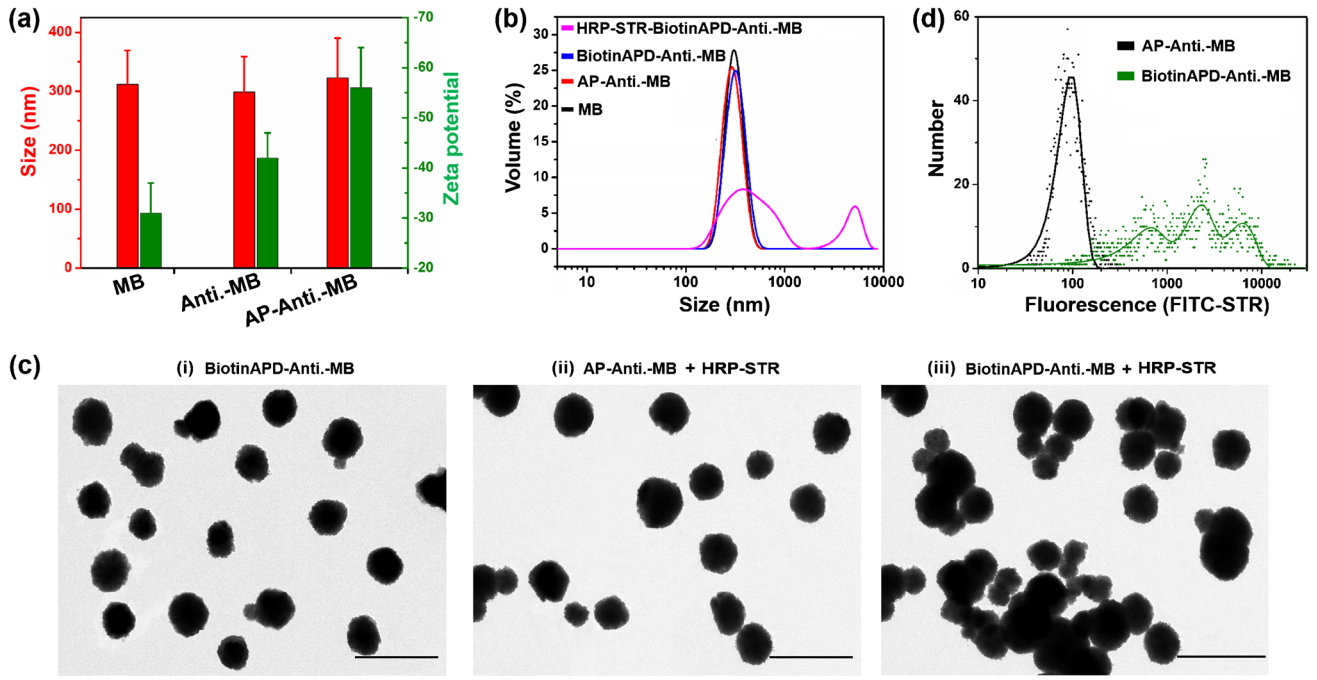

Fig. 4 Characterization of on-bead DNA synthesis. (a) The size and zeta potential of the magnetic beads (MBs) with and without modifications. (b) Representative size distribution of the MBs with various modifications. (c) TEM images of the MBs with and without DNA synthesis. (i) The beads with DNA synthesis were directly observed by TEM. (ii) The beads without DNA synthesis were incubated with HRP-STR and were observed by TEM. (iii) The beads with DNA synthesis were incubated with HRP-STR and were observed by TEM. The scale bar is 500 nm. (d) Flow cytometry analysis of the MBs carrying biontin-dsDNA after FITC-STR staining. Abbreviation: Anti.-MB, Antibody conjugated MB; AP-Anti.-MB; AP conjugated Anti.-MB; BiotinAPD-Anti.-MB, AP-Anti.-MB after on-bead DNA synthesis; HRP-STR-BiotinAPD-Anti.-MB, BiotinAPD-Anti.-MB incubated with HRP-STR

11 bp, the AP-Anti.-MB (AP conjugated MB) without CEA showed fade green fluorescence (Fig. 5 b1). In the presence of CEA, on-bead DNA synthesis was initiated. As a result, the AP-Anti.-MB showed enhanced green fluorescence upon SYBR Green staining (Fig. 5 c1 and d2) and red fluorescence upon PE-AF 647-STR staining (Fig. 5 c2 and d2). When 80 ng/mL CEA was used to initiated DNA synthesis, many AP-Anti.-MBs tended to aggregate due to the binding of PE-AF647-STR with biotin-dsDNAs at multiple sites on the beads (Fig. 5 d2), which was consistent with that observed by TEM (Fig. 4c) and FCM (Fig. 4d). These results further verify the successful on-beads DNA synthesis and the insertion of biotin molecules into the on-beads dsDNA.

Quantitative detection of CEA by APMB system

To investigate the quantifiability of the approach, a series of CEA standard solutions were prepared and subjected to APMB analysis. Figure 6a showed the UV–visible absorption spectra of the oxidized TMB produced by catalytic reaction of HRP-STR on the beads. The absorbance is directly proportional to the CEA concentration, and even 0.05 ng/mL could be recognized from the background. Since the oxidized TMB shows absorption peak at 450 nm, the absorbance at this point (OD_{450}) was used as sensor signal for the subsequent experiments.

The amount of MB used for target separation and biosensing was optimized to improve the assay performance. As shown in Fig. 6b, both signal and background increased with the increase of MB dose. Low MB doses were insufficient to capture abundant targets for subsequent amplification, leading to low S/N ratios. On the other hand, too much MB and AP conjugated with it could result in nonspecific DNA synthesis and amplification, which also contributed to the low S/N ratio. The optimal MB dose was 25 ug, as it obtained a highest S/N ratio for detecting 80 ng/mL CEA. Figure 6c showed the dynamic responses of the absorbance (OD_{450}) to the CEA concentration change. By running the DNA synthesis on beads for 35 min, the detection limit could be lowered to 0.01 ng/mL (Fig. 6c and Supplementary Fig. S3). Hence, the sensitivity can be greatly improved through on-bead DNA synthesis triggered by the AP and target protein.

Figure 6d and e showed the quantifiability of the APMB system for CEA detection. The OD_{450} increased linearly with the CEA concentration in the range of 0.05 to 20 ng/mL. There is a good correlation between the CEA concentration and the OD_{450} value measured by APMB, with a correlation coefficient R^2 of 0.9211. The CEA

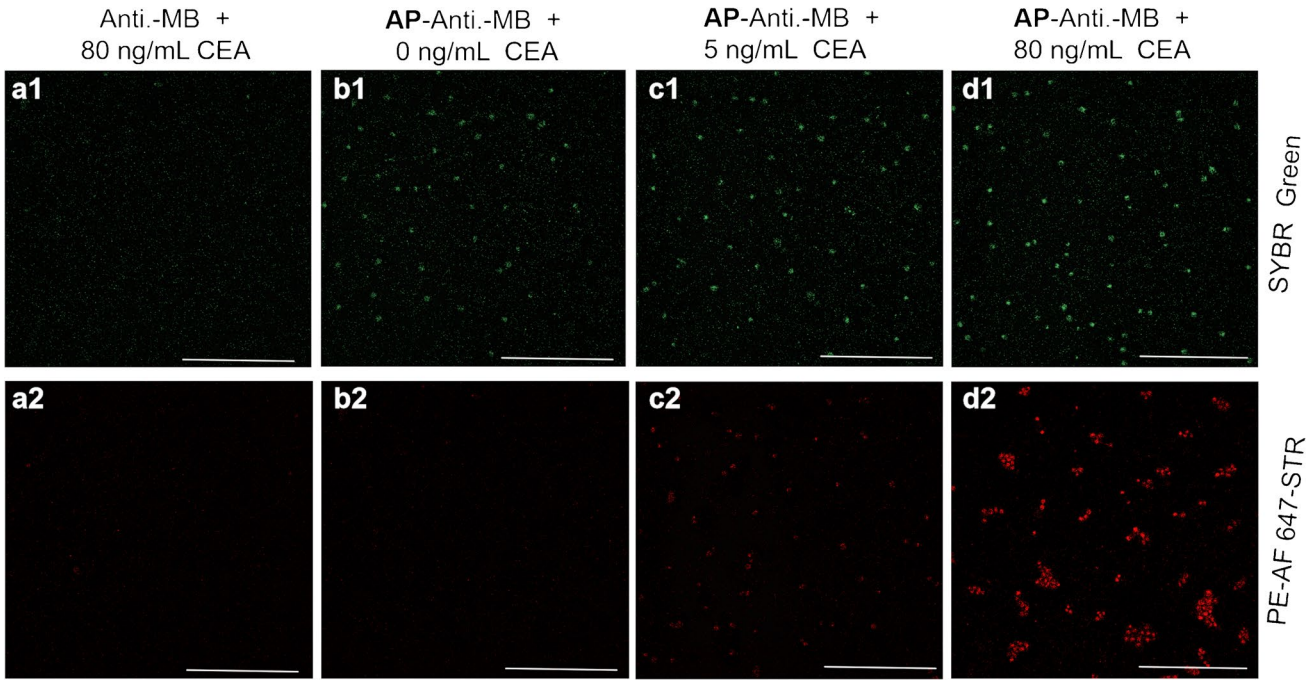

Fig. 5 Fluorescent images of the MBs after on-bead DNA synthesis. (a) As a control, antibody-conjugated MBs were incubated with 80 ng/mL CEA to initiate DNA synthesis. (b–d) AP conjugated MBs were incubated with 0, 5, and 80 ng/mL CEA, respectively, to initiate DNA synthesis. The beads were stained with SYBR Green targeted to double-stranded DNA (a1–d1) and PE-AF 647-STR targeted to biotin labeled DNA (a2–d2), respectively. The scale bar is 10 μm

concentrations of clinical serum may range from 0.1 to 1000 ng/mL [29]; for CEA values above 20 ng/mL, the serum could be diluted into pure water for further determination. Compared with traditional ELISA for CEA quantification, the present method increases the detection sensitivity by 100-fold and cuts the detection time from two hours to about 70 min, as shown in Fig. 6f. These results demonstrate high sensitivity, good quantifiability and high efficiency of the APMB for protein quantification.

Practicability of the APMB system for clinical sample detection.

Figure 7a showed the specificity of the APMB evaluated by using interferents that are commonly found in serum or bioexperiment. The as-developed APMB was selective to target protein, and no comparable signals were observed for interferents. Therefore, the good specificity of APMB for the tested CEA concentration (0.05 ng/mL) was demonstrated. To further investigate the practicability of the APMB system for clinical sample detection, both ELISA and APMB were carried out to detect clinical samples from a healthy donor, with ten duplicated assays for each method. As shown in Fig. 7b, although there was no significant difference in detected average value between the two methods, APMB demonstrated a much better performance for its excellent repeatability in quantifying CEA of low content.

The critical value of CEA in human serum is commonly set as 5 ng/mL, exceed which would be regarded as a suspected tumor patient. Currently, ELISA maintains the most widely used method for CEA testing in hospitals. Since the detection limit of ELISA is near the diagnostic critical value, false negatives or false positives inevitably occurred due to the erratic fluctuation as shown in Fig. 7c. In contrast, with high sensitivity, the APMB shows a more precise and repeatable result for detecting CEA lower than 5 ng/mL. Additionally, the APMB showed no reduction in responsive absorbance and signal-to-background ratio within 30 days, as shown in Supplementary Fig. S4, illustrating good stability of the APMB for practical applications.

Conclusion

The ability to detect protein biomarkers of low concentrations in clinical samples remains a great challenge. Here, we established an on-bead DNA synthesis system (named APMB) that can determine very low concentrations of a protein biomarker by using allosteric probe (AP) combined with magnetic bead (MB). The protocol for on-bead DNA synthesis was optimized to obtain the optimal AP, primer, temperature, biotin-dATP content, and MB dose. Under the optimum conditions, the hairpin AP could be successfully

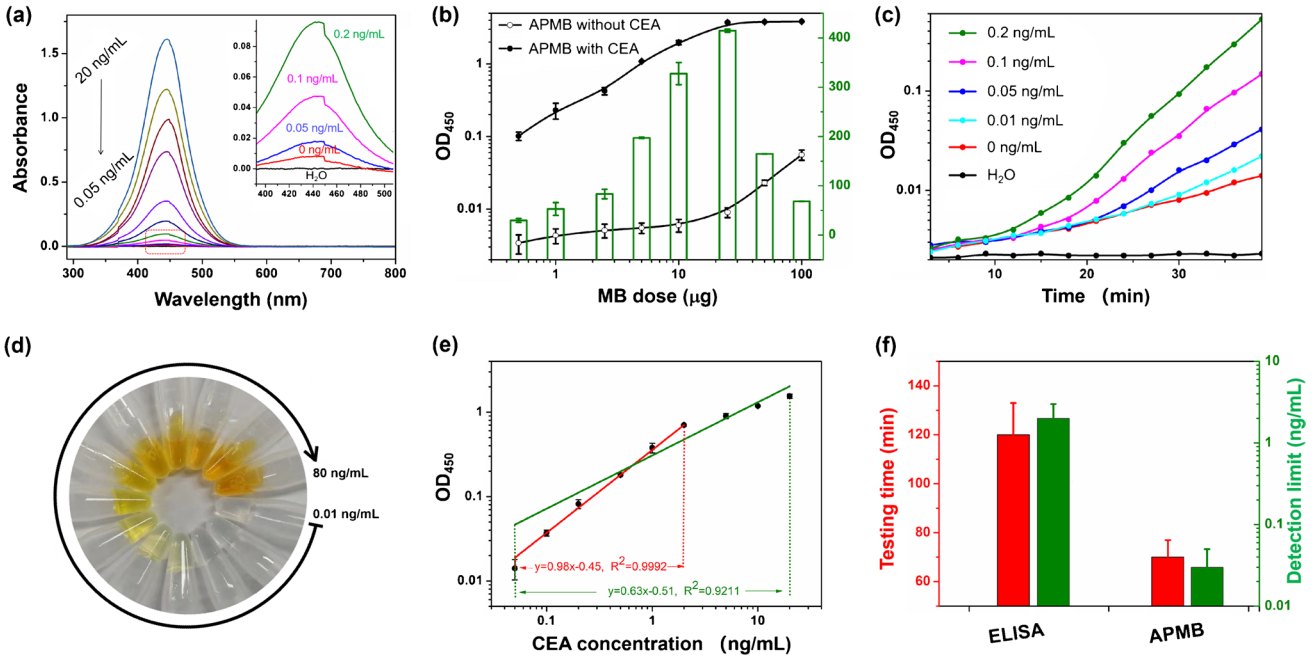

Fig. 6 Quantification of CEA by APMB. (a) UV–visible absorption spectra of the oxidized TMB produced by catalytic reaction. (b) The effect of MB dose on the signal-to-background ratio (S/N) of the APMB system for detecting 80 ng/mL CEA. The S/N was defined as the ratio of OD_{450} value of APMB with CEA to that without CEA after color reaction. (c) The dynamic responses of OD_{450} value to the CEA (ranging from 0 to 0.2 ng/mL) along with the progress of DNA synthesis. Two samples, one without CEA (0 ng/mL) and the other without AP (use H_2O instead), were set as controls. (d) Colorimetric observation of the APMB results. (e) Linear analysis of CEA detection by APMB. Red line and green line represent linear regression analyses for CEA concentration ranging from 0.05 to 2 ng/mL (red) and 0.05 to 20 ng/mL (green), respectively. (f) Comparison of APMB system and conventional ELISA with respect to detection time and limit

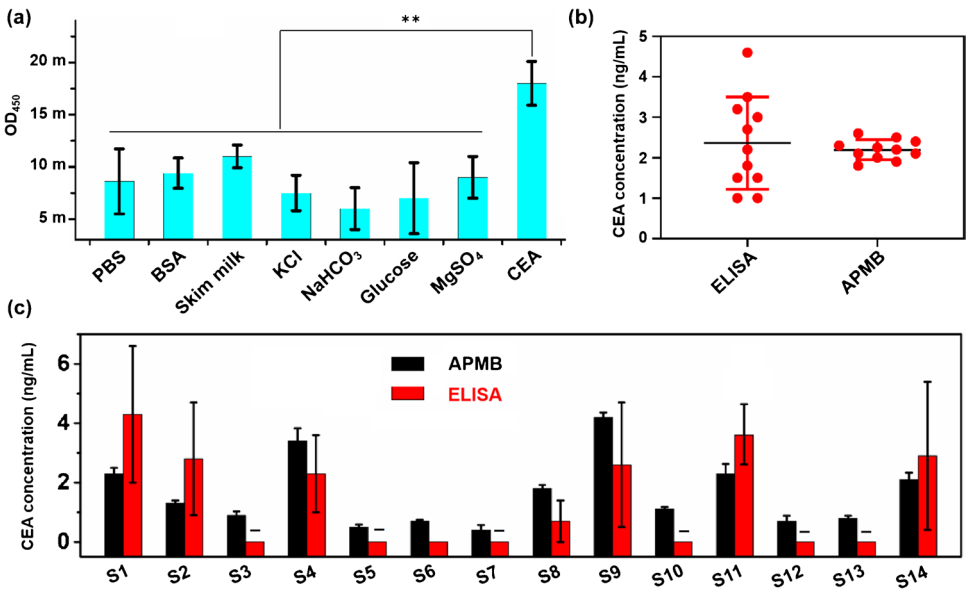

Fig. 7 Specificity and practicability of the APMB system for CEA detection. (a) Selective response of the APMB system to 0.05 ng/mL CEA against other common interferents. The concentrations of the interferents were as encountered in the serum [30]. The differences in OD_{450} between the CEA and interferents are significant, as indicated with two asterisks ($p < 0.01$). (b) Precision comparison of the APMB and ELISA for CEA detection of clinical samples from a donor. (c) Comparison of the APMB and ELISA for CEA detection of clinical samples from 14 donors. Five independent analyses were carried out for each method. Subtraction signs represent the CEA concentrations were below the limit of detection, and were marked as 0 ng/mL. S1–S14, Sample 1 to Sample 14

unfolded in response to target protein, initiating the on-bead DNA synthesis for primary amplification. During the DNA synthesis, biotin-dATP tag was successfully incorporated into the DNA. The DNA was recognized by HRP-STR, which catalyzed colorimetric reaction for secondly amplification. By using CEA as a model protein biomarker, the APMB showed about two orders of magnitude more sensitive than traditional ELISA, and cut the detection time from 120 to 70 min. Future researches may focus on the assembling of APMB system targeted to protein biomarkers that are present in saliva or urine at pg/mL level to facilitate noninvasive and early diagnoses.

Supplementary Information The online version contains supplementary material available at https://doi.org/10.1007/s00604-022-05404-4.

Author contribution **Min Ling:** Investigation, Writing, Funding acquisition. **Na Luo and Lanyu Cui:** investigation, Data curation. **Yongqiang Cao, Xueping Ning, Jian Sun, and Xiaoping Xu:** Investigation, Data curation, Writing- review & editing. **Shengbin He:** Conceptualization, Writing-review & editing, Validation, Supervision, Project administration, Funding acquisition.

Funding This research was supported by the Guangxi Natural Science Foundation (Grants 2021JJB130333), National Natural Science Foundation of China (Grants 81260245), and Middle-aged and Young Teachers' Basic Ability Promotion Project of Guangxi (Grants 2020KY03011), for which we are most grateful.

Declarations

Conflict of interest The authors declare no competing financial interests.

References

1. Slavov N (2020) Unpicking the proteome in single cells. Science 367(6477):512–513
2. Singh A (2021) Subcellular proteome map of human cells. Nat Methods 18(7):713–713
3. Pan Z, Yang D, Lin J, Shao K, Shi S, Teng YJ, Liu H, She Y (2022) Autofluorescence free detection of carcinoembryonic antigen in pleural effusion by persistent luminescence nanoparticle-based aptasensors. Anal Chim Acta 1194:339408
4. Sun J, Ning X, Cui L, Ling M, He S (2020) Assembly of "carrier Free" enzymatic nano-reporters for improved ELISA. Analyst 145(20):6541–6548
5. Wang YR, Chuang HC, Tripathi A, Wang YL, Ko ML, Chuang CC, Chen JC (2021) High-sensitivity and trace-amount specimen electrochemical sensors for exploring the levels of beta-amyloid in human blood and tears. Anal Chem 93(22):8099–8106
6. Liu Y, Hao L, Wang W, Yang H, Si F, Kong J (2021) Functionalized graphene oxide in situ initiated ring-opening polymerization for highly sensitive sensing of cytokeratin-19 fragment. Microchim Acta 188(4):123
7. Gao M, Daniel D, Zou HY, Jiang S, Lin S, Huang C, Hecht SM, Chen S (2018) Rapid detection of a Dengue virus RNA sequence with single molecule sensitivity using tandem toehold-mediated displacement reactions. Chem Commun 54(8):968–971
8. Gao M, Waggoner JJ, Hecht SM, Chen S (2019) Selective detection of Dengue virus serotypes using tandem toehold-mediated displacement reactions. ACS Infect Dis 5(11):1907–1914
9. Ravi N, Cortade DL, Ng E, Wang SX (2020) Diagnostics for SARS-CoV-2 detection: a comprehensive review of the FDA-EUA COVID-19 testing landscape. Biosens Bioelectron 165:112454
10. Ganguli A, Mostafa A, Berger J, Aydin M, Sun F, Valera E, Cunningham B, King WP, Bashir R (2020) Rapid isothermal amplification and portable detection system for SARS-CoV-2. Proc Natl Acad Sci USA 117(37):22727–22735
11. Mollarasouli F, Zare-Shehneh N, Ghaedi M (2022) A review on corona virus disease 2019 (COVID-19): current progress, clinical features and bioanalytical diagnostic methods. Microchim Acta 189(3):103
12. Ruan X, Liu D, Niu X, Wang Y, Simpson CD, Cheng N, Du D, Lin Y (2019) 2D graphene oxide/Fe-MOF nanozyme nest with superior peroxidase-like activity and its application for detection of woodsmoke exposure biomarker. Anal Chem 91(21):13827–13854
13. Yang YC, Liu MH, Yang SM, Chan YH (2021) Bimodal multiplexed detection of tumor markers in non-small cell lung cancer with polymer dot-based immunoassay. ACS Sens 6(11):4255–4264
14. Tan X, Chen Q, Zhu H, Zhu S, Gong Y, Wu X, Chen Y, Li X, Li MW, Liu W, Fan X (2020) A fast and reproducible ELISA laser platform for ultrasensitive protein quantification. ACS Sens 5(1):110–117
15. Kim HS, Lee T, Yun J, Lee G, Hong Y (2021) Cancer protein biomarker identification and quantification using nanoforest substrate and hand-held Raman spectrometer. Microchem J 160:105632
16. Sun J, Mao Y, Cui L, Cao Y, Li Z, Ling M, Xu X, He S (2021) Using a safe and effective fixative to improve the immunofluorescence staining of bacteria. Methods Appl Fluores 9(3):035001
17. Tyrrell DA, Campbell PI, Harding NGL, Munro A, Ryman BE (1978) Anti-digoxin antibody incorporation into liposomes: a potential therapy for digoxin toxicity. Biochm Soc Trans 6(6):1239–1241
18. Shen J, Zhou X, Shan Y, Yue H, Huang R, Hu J, Xing D (2020) Sensitive detection of a bacterial pathogen using allosteric probe-initiated catalysis and CRISPR-Cas13a amplification reaction. Nat Commun 11(1):1–10
19. Cheng K, Zhou J, Shao Z, Liu J, Song J, Wang R, Li J, Tan W (2020) Aptamers as versatile molecular tools for antibody production monitoring and quality control. J Am Chem Soc 142(28):12079–12086
20. Zhang B, Wang X, Cheng Y (2022) Photochromic immunoassay for tumor marker detection based on ZnO/AgI nanophotocatalyst. Microchim Acta 189(2):77
21. Ganesan S, Venkatakrishnan K, Tan B (2020) Wrinkled metal based quantum sensor for In vitro cancer diagnosis. Biosens Bioelectron 151(2):111967
22. Yang Y, Hu G, Liang W, Yao L, Huang W, Zhang Y, Zhang J, Wang J, Yuan R, Xiao D (2020) An AIEgen-based 2D ultrathin metal–organic layer as an electrochemiluminescence platform for ultrasensitive biosensing of carcinoembryonic antigen. Nanoscale 12(10):5932–5941
23. Tabar HG, Smith C (2010) DNA Aptamers selected as a molecular probe for diagnosis of cancerous cells. World Appl Sc J 8(1):16–21
24. Wang P, Wan Y, Deng S, Yang S, Su Y, Fan C, Aldalbahi A, Zuo X (2016) Aptamer-initiated on-particle template-independent enzymatic polymerization (aptamer-OTEP) for electrochemical analysis of tumor biomarkers. Biosens Bioelectron 86:536–541
25. Qi L, Liu S, Jiang Y, Lin JM, Yu L, Hu Q (2020) Simultaneous detection of multiple tumor markers in blood by functional liquid crystal sensors assisted with target-induced dissociation of aptamer. Anal Chem 92(5):3867–3873

26. Zhang R, Liu L, Mao D, Luo D, Cao F, Chen Q, Chen J (2020) Construction of electrochemical aptasensor of carcinoembryonic antigen based on toehold-aided DNA recycling signal amplification. Bioelectrochemistry 133:107492
27. Albani JR (2007) Principles and applications of fluorescence spectroscopy. Wiley-Blackwell
28. Lakshmipriya T, Gopinath SCB, Tang T (2016) Biotin-streptavidin competition mediates sensitive detection of biomolecules in enzyme linked immunosorbent assay. PLoS ONE 11(3):e0151153
29. Haagensen DE, Cox CE, Dilley WG, Hensley M, Murdoch J, Newman ES, Wells SA (1980) Evaluation of baboon antiserum to carcinoembryonic antigen. Clin Chem 26(13):1787–1790
30. Alex SA, Chandrasekaran N, Mukherjee A (2018) Gold nanorod-based fluorometric ELISA for the sensitive detection of a cancer biomarker. New J Chem 42(19):15852–15859